

Metal localization in water hyacinth roots from an urban wetland

P. A. VESK¹, C. E. NOCKOLDS² & W. G. ALLAWAY¹

¹School of Biological Sciences and ²Electron Microscope Unit, The University of Sydney, NSW 2006 Australia

ABSTRACT

Metal localization within and around roots of water hyacinth (*Eichhornia crassipes*) growing in a wetland receiving urban run-off was studied by energy dispersive X-ray microanalysis of sections from freeze-substituted roots. Sampling randomly from an order of magnitude gradient in metal concentrations (Cu and Pb) allowed us the opportunity to identify general patterns of metal localization. Iron was present at high levels at the root surface, and this may have been a root plaque as described for wetland plants with roots anchored in flooded soils. Iron levels decreased centripetally across the root and were higher in cell walls than within cells. Trace metals (Cu, Zn and Pb) were not localized at the root surface. In contrast with iron, trace metal levels increased centripetally across the root, tended to be higher inside cells and were highest within cells in the stele. Variability of localization was high for all metals analysed. Multivariate statistical analyses (principal components analysis and multidimensional scaling) were useful for identifying overall patterns in elemental distribution.

Key-words: *Eichhornia crassipes* (Mart.) Solms; accumulation; copper; iron; lead; multivariate analysis; root plaque; uptake; X-ray microanalysis; zinc.

Abbreviations: PCA, principal components analysis; MDS, multidimensional scaling; STEM, scanning transmission electron microscopy.

INTRODUCTION

Aquatic plants are known to accumulate metals from their environment (Outridge & Noller 1991) and affect metal fluxes through those ecosystems (Jackson, Rasmussen & Kalff 1994; St-Cyr, Campbell & Guertin 1994). These effects have led scientists, engineers and managers to be interested in metal toxicity and tolerance (van Steveninck *et al.* 1990a; Ernst, Verkleij & Schat 1992), and the roles of aquatic plants in biogeochemical metal fluxes (Jackson *et al.* 1994; St-Cyr *et al.* 1994), as biological filters for polluted waters (Brix & Schierup 1989; Ellis *et al.* 1994); and as biomonitors of environmental metal levels (Whitton & Kelly 1995; Markert 1995).

Correspondence: Peter A. Vesk, Electron Microscope Unit F09, The University of Sydney, NSW 2006 Australia. Fax: 61 2 93517682; e-mail: peter@emu.usyd.edu.au

Metal accumulation is of interest for basic research into the physiology and ecology of plant survival in flooded conditions and under elevated metal levels (Otte *et al.* 1989). Root plaques, predominantly of Fe, are commonly found on wetland plants with anchored roots and conflicting results have been reported as to their effects on metal uptake, immobilization and tolerance (Otte *et al.* 1989; St-Cyr & Campbell 1996; Ye *et al.* 1997). X-ray microanalysis has been suggested as a way to investigate these questions further (Ye *et al.* 1997).

Despite much work, there are no clear guidelines for biomonitoring of metals using aquatic plants (Langston & Spence 1994; Phillips 1994; Markert 1995). The surface layer of roots may be enriched in metals but not be bioavailable; further it may affect uptake of metals (Markert 1995; St-Cyr & Campbell 1996). There are many instances where wetlands-utilizing aquatic plants are employed for removal of pollutants, including metals, from waters (see Brix & Schierup 1989; Dunbabin & Bowmer 1992; Ellis *et al.* 1994). Considerable information exists on the influence of aquatic plants on metal fluxes at larger scales, indeed many studies take a black box approach, focusing on influent and effluent pollutant concentrations. Additionally, small scale laboratory research has addressed the kinetics of metal uptake by plants (e.g. Lee & Hardy 1987; Thornton & Macklon 1989; Brune, Urbach & Dietz 1994). However, less is known about small scale patterns and processes of metal accumulation in the field and, importantly, how these might affect larger scales. The extent to which metals are taken up and how they are distributed within plants may have important consequences for the capacity and rate of metal uptake, the metal residence time in plants and wetlands and the eventual release of metals. To improve understanding of the importance and roles of aquatic plants, we must investigate metal uptake and localization (Ellis *et al.* 1994).

This article reports the localization of metals in the roots of free-floating water hyacinth *Eichhornia crassipes* (Mart.) Solms, from an urban wetland in Centennial Park, Sydney, Australia. In a previous paper we reported that concentrations of Cu and Pb in the roots of water hyacinth from this wetland declined by more than an order of magnitude over a distance of 500 m downstream from an inflow (Vesk & Allaway 1997). Compared with other reports, root concentrations of Pb were generally high at all sites sampled (145 ± 15 to $1110 \pm 145 \mu\text{g g}^{-1}$ dry mass) and root Cu concentrations ranged from relatively low to relatively high (14.7 ± 7.0 to $303 \pm 108 \mu\text{g g}^{-1}$ dry mass)

(mean \pm sd, $n = 6$ plants at each site) (Vesk & Allaway 1997). In the present study we sought to identify and describe general patterns of metal localization in roots by randomly sampling along this gradient of metal concentrations. This was to cover a range of concentrations that might allow some extrapolation to the wider environment (Beck 1997) and also so that metal levels would be sufficient for detection. X-ray microanalysis was performed on freeze-substituted secondary roots which are the site of the highest concentrations of Pb and Cu (Vesk & Allaway 1997). Considering the possibility that the root surface was the major site of metal accumulation, we addressed the hypotheses that: (a) metal levels (Fe, Cu, Zn and Pb) were highest at the root surface, outside the root; (b) there was a decreasing gradient of metal levels towards the stele; (c) cell walls had greater metal levels than the cell interiors; (d) metals differed in their patterns of distribution.

MATERIALS AND METHODS

Site and plants

The site and metal concentrations of roots and leaves and sediments are reported in a previous publication (Vesk & Allaway 1997) so are only presented briefly here. Kensington Pond in Centennial Park, Sydney receives runoff from an urban catchment that includes residential, commercial and intensive recreational use including major roads. Within a linear arm of this wetland a dense raft of free-floating water hyacinth, *Eichhornia crassipes* (Mart.) Solms, extended over a downstream transect, roughly 500 m long, from an inflow drain. Well-established plants were sampled at random distances along this transect in water about 1 m deep, 2–4 m from the banks on 19 March 1995. A long primary root (> 20 cm long) with attached laterals was cut from each plant and taken to the laboratory in a polythene bag with a small amount of pond water. In the laboratory lateral roots 10–20 mm long and about 200 μm diameter were cut from the main root for subsequent plunge freezing.

Specimen preparation

Many studies have shown how elements are lost and redistributed using conventional aqueous preparation, e.g. fixation with glutaraldehyde, osmium tetroxide post-fixation, wet sectioning (e.g. Morgan 1980; Mullins, Hardwick & Thurman 1985; Vázquez *et al.* 1992; Orlovich & Ashford 1995). We therefore used anhydrous freeze-substitution methods which have been recommended for X-ray microanalysis studies of plant tissues (Mullins *et al.* 1985; Vázquez *et al.* 1992; Orlovich & Ashford 1995). The roots were plunge frozen by hand in liquid propane cooled by liquid nitrogen. Following storage in liquid nitrogen, the roots were freeze-substituted in anhydrous diethyl-ether, basically following the method of Orlovich & Ashford (1995). Substitution lasted 10 weeks at 193 K, specimens were warmed to 253 K, left overnight, warmed to 273 K, left overnight again and brought to room temperature.

Further processing was carried out in a dry nitrogen-flushed glove box (Marshall 1980). The roots were infiltrated with 30% Spurr's resin in ether over 48 h, the resin concentration increased to 100% and the samples left 24 h before flat embedding in fresh resin. Specimens were then polymerized at 333 K over 48 h. Semi-thin (0.5 μm) transverse sections about 1 mm back from the root tip were cut on a dry glass knife and sandwiched between a carbon-coated parlodion film and a formvar film on a nickel slot grid. Grids were stored in grid boxes in a desiccator awaiting analysis, usually on the same day.

Microscopy and X-ray microanalysis

Unstained sections were examined with a Philips (Eindhoven, the Netherlands) CM12 Scanning Transmission Electron Microscope (STEM) at 120 kV using a LaB₆ emitter. Energy dispersive X-ray microanalysis was carried out with the same microscope, equipped with a thin Be window detector and DX4 multichannel analyser (Edax, Mahwah, NJ, USA). Specimen tilt was 20° using a Be low background holder. Beam current was typically 1.5–2.5 nA indirectly measured with a spray current meter connected to condenser aperture two and calibrated with a Faraday cup. Analyses were made in STEM mode using a reduced area scan within the desired region, ranging from 0.05 μm^2 to 2.60 μm^2 . We estimated lateral spread of the beam from the scanned areas using Monte Carlo calculations (Joy 1995) for two cases. Firstly, cell wall analyses which were typically rectangular, 0.4 $\mu\text{m} \times 2.0 \mu\text{m}$, for which we assumed a pure carbon film 0.5 μm thick with density 2.34 g m⁻²; 90% of electron interactions occurred within about 32 nm radius around the incident beam leading to a small inflation in the dimensions of the scan. In the second case of solid granules, for example, Fe-rich granules, we assumed Fe₂O₃, density 5 g m⁻²; 90% of interactions would be located within 86 nm radius around the incident spot. However, electrons scattered into the surrounding low density matrix would contribute little to the X-ray signal.

Two analyses were made at each of seven regions on one section from each of two roots from each of 18 plants. The seven regions were: external granules; epidermis external wall; epidermis internal wall; parenchyma internal wall; stele wall; epidermis cytoplasmic granules; and stele cytoplasmic granules. These regions were chosen based on the distribution of Fe observed from preliminary X-ray microanalyses. Cytoplasmic granules were defined as anything intracellular that yielded electron contrast in these unstained, anhydrously prepared sections. This meant that no distinction was possible between free and bound elements, nor whether they were in cytoplasm, vacuoles or other organelles. Plunge freezing roots about 200 μm in diameter led to ice crystal formation. This would have contributed in part to formation of at least some of the observed granules. Cells of the stele included xylem vessels, parenchyma and phloem. These were not distinguishable, and so analyses of stele cytoplasmic granules might include xylem vessels which are not symplastic.

Spectra were collected over 100 live seconds except in some cases where count rates were very low which resulted in high detector dead time (a quirk of this particular detector). In such cases 120 clock seconds were used (the typical time taken for a standard analysis) to avoid extremely long analyses. Spectra were processed by fitting a standard background, fitting peaks and calculating net X-ray intensities for the elements: Na, Mg, Al, Si, P, S, K, Ca, Ti, Mn, Fe, Cu, Zn and Pb. Peaks were fitted for Cl and Ni, but their intensities used no further as Cl was present in the resin and Ni was the material of the support grid. Average spectra for the different root regions analysed were constructed using DTSA (Desk Top Spectrum Analyzer, US National Institute of Standards and Technology, Gaithersburg, MD, USA) using grand means of net elemental X-ray intensities. Iron X-ray maps were made by recording X-ray counts in a window of 120 eV around 6.4 keV, with a dwell time of 100 ms in a 128 × 100 pixel array.

Semi-thin sections for light microscopy were stained with toluidine blue. Specimens for scanning electron microscopy were freeze-substituted at 193 K over 3 d with acetone and warmed to 253 K, left overnight, warmed to 277 K for 4 h then brought to room temperature, rinsed with fresh acetone twice, frozen in liquid nitrogen and freeze-dried. Specimens were then coated with 3 nm of Pt and observed in a Jeol (Tokyo, Japan) 6000F scanning electron microscope at 5 kV.

Statistical analyses

To remove total count variation due to specimen density, section thickness and beam current variation, proportional data were generally used (except for principal components analysis, see below). Use of proportional data also removed any effect of variation in the length of analysis time. Net X-ray intensities for each element were divided by the sum of elemental intensities (excluding Cl and Ni). Dividing net X-ray intensities by the beam current measured by the condenser aperture spray meter was tried to remove some variation, with little success. The use of proportional data in this study compared with normalization by beam current slightly biased the levels of elements in the stele walls and parenchyma internal walls upward, and elemental levels in external granules and epidermal cytoplasmic granules downward, particularly for elements with highly skewed frequency distributions such as Fe, Zn, Cu and Al.

Data for individual metals were analysed by three-way analyses of variance. Generally the analyses of variance (not shown) were dominated by interactions at the levels of regions by roots nested in plants or regions by plants. This meant that patterns were not consistent among roots or among plants and highlighted the small scale variability. Plots of mean element proportions were made with pooled standard errors which were back-transformed to the original scale (Clarke & Green 1988).

We used multivariate data analysis to identify and interpret patterns in these complex multi-element data sets. We used SAS software (version 6, SAS Institute Inc Cary, NC USA) for correlation-based principal components analysis

(PCA). This analysis identified a small number of uncorrelated linear combinations of elements which maximized variance in the data set, and hence 'explained' variation (Manly 1994; Norman & Streiner 1994). This can be understood as combining those elements that varied the most in a similar fashion into a new 'dimension' of the data. This is carried out successively with the elements which vary to lesser degrees with the aim of being left with fewer dimensions to describe the data. PCA was carried out on a reduced data set using means of net X-ray intensities for the four analyses for each region from each plant. These data ($n = 7$ regions × 18 plants = 126) were transformed by $x' = \log_e(x + 0.001)$. Cattel's scree test was used to identify how many factors to retain (Norman & Streiner 1994). This was followed by varimax rotation. We determined the significant factor loadings using a conservative critical value for correlation of twice the level of $\alpha = 0.01$ (Norman & Streiner 1994). Ordination of samples with PCA resulted in little of the variation being represented in a two dimensional plot. PCA was however, useful in revealing the 'principal components' or linear combinations of similarly distributed elements. Multi-element variation was represented in two dimensions by plotting samples using non-metric multidimensional scaling (MDS) (Kruskal & Wish 1978; Clarke 1993; Manly 1994) with PRIMER software (Plymouth Marine Laboratories UK). This MDS ordination used Bray-Curtis similarities calculated from proportional data that were then fourth-root transformed (Clarke 1993). The MDS ordination space was interpreted by multiple linear regression of the principal component scores for each sample (calculated using the factor loading) on the x and y co-ordinates of the samples in the ordination (Kruskal & Wish 1978). After testing the regressions for statistical significance with an F -ratio test, arrows representing the principal components were plotted on to the MDS ordination.

RESULTS

The root surface was often covered with a reddish to brown layer. This included mucilage, particulates such as clays, and a diversity of micro-organisms including bacteria, protozoans and diatoms (Fig. 1). Preliminary X-ray microanalysis revealed high levels of Fe, particularly at the root surface, in electron opaque deposits within cells and in cell walls. An X-ray map illustrates this Fe distribution (Fig. 2). X-ray maps of the trace metals were not made due to their low concentrations. Subsequently, more extensive sampling was designed to investigate the localization of Fe and other metals, particularly Cu, Pb and Zn, among regions of transverse sections of lateral roots (Fig. 3).

Spectra modelled from mean X-ray intensities for the various regions roughly indicate patterns of elemental localization (Fig. 4). In addition to Fe, external granules at the root surface were also characterized by high Si and Al indicating clay particles, and Ti and Mn were also present in lower concentrations (Fig. 4a). The Fe peak decreased in size in successive cell walls from the epidermal external



Figure 1. Scanning electron micrographs of the surface of water hyacinth roots from Kensington Pond. a, Note the root epidermal cell outlines (arrowheads) underlying mucilage, micro-organisms and clay particles. Some cells appear collapsed and filled with granular material. Bar = 10 μm . b, Higher magnification, illustrating individual bacteria (arrowheads) and a clay particle (arrow). Bar = 2 μm .

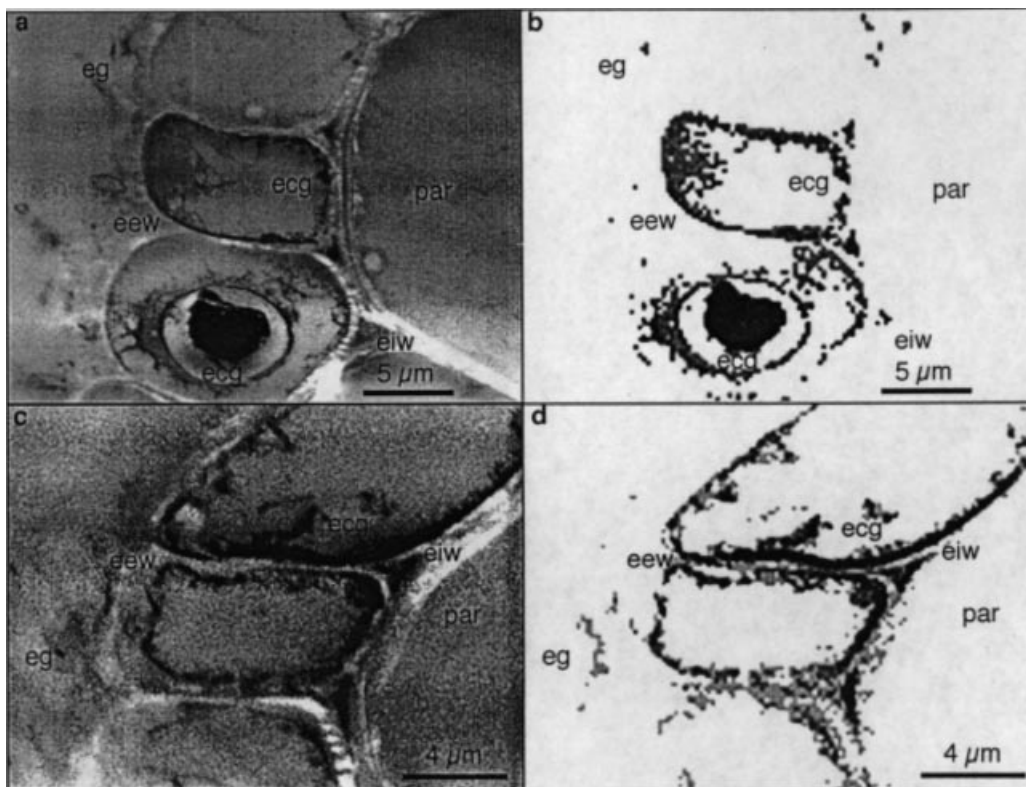


Figure 2. Scanning transmission electron microscopy images (a and c) and corresponding X-ray maps of Fe distribution (b and d) around the epidermis of water hyacinth lateral roots. In (b) and (d), black is high Fe concentration, white is absence of Fe; eg, external granules; eew, epidermis external wall; eiw, epidermis internal wall; ecg, epidermis cytoplasmic granules; par, parenchyma.

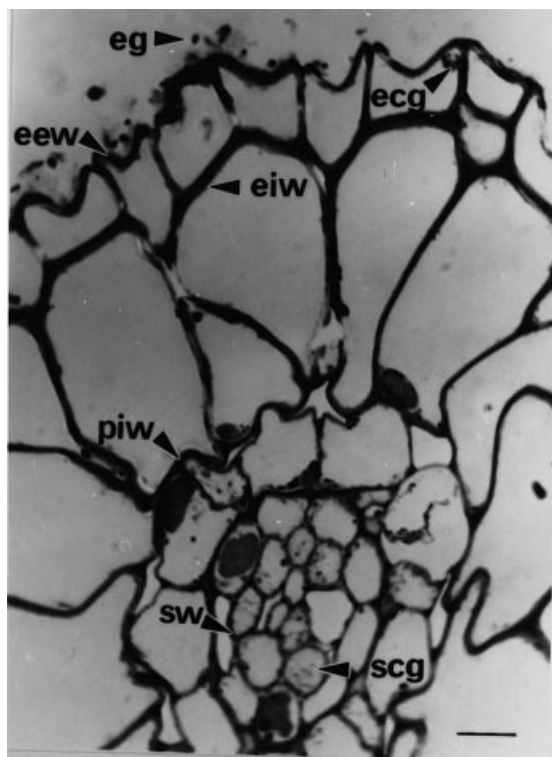


Figure 3. Light micrograph of a transverse section of a lateral root of water hyacinth, toluidine blue staining. The regions selected for X-ray microanalysis are indicated (eg, external granules; eew, epidermis external wall; eiw, epidermis internal wall; piw, parenchyma internal wall; sw, stele internal wall; ecg, epidermis cytoplasmic granules; scg, stele cytoplasmic granules). Bar = 10 μm .

walls through to the stele walls (Figs 4b–e). A large Fe peak was present in epidermal cytoplasmic granules (Fig. 4f) but absent from stele cytoplasmic granules (Fig. 4g). The stele cytoplasmic granules were the only obvious location of Cu and Zn (Fig. 4g), and substantial peaks of P, S and K can also be seen in this spectrum and the spectrum from epidermal cytoplasmic granules (Fig. 4f).

Principal components analysis (PCA) displayed only 34% of the variation in the first two dimensions (Table 1), and therefore we have not presented PCA plots here. PCA did, however, identify combinations of elements that were distributed similarly (Table 1). The first principal component (PC1) represented Si, Al and Ti, and explained the largest proportion of the variation in the data (Table 1). The second most important component (PC2) contrasted variation of Cu and Zn with that of Fe (Table 1). The first four principal components were useful in interpreting the multidimensional scaling (MDS) plot as described below.

A two-dimensional MDS plot, representing similarity among individual analyses, is shown in Fig. 5. There was considerable overlap among regions of the root displayed in the MDS plot (Fig. 5a), although there were discernible patterns: external granules can be seen in the lower centre of the ordination, epidermal walls at lower left, and stele

analyses at top right. These patterns were more clearly seen when only the region centroids were plotted (Fig. 5b). The axes of the MDS plot have no intrinsic meaning in terms of elements, however, so the principal components were used to interpret the MDS ordination (Table 1 and Fig. 5b).

We used multiple regression of the principal component scores on the x and y co-ordinates of the MDS plot for each sample. An *F*-ratio test found that the first four principal components explained patterns in the MDS plot at a high level of statistical significance (Table 1). Arrows representing these four principal components are plotted on Fig. 5b. From these it can be seen that moving from external granules through epidermis external walls into the root (from bottom right towards top left of the ordination) corresponds to a decrease in PC1 and a concomitant increase in PC4. In other words Si, Al and Ti (indicative of clay particles) decreased in this inward direction, while K, Mg and Na increased. This drew a clear distinction between the root surface and the root interior.

In a different direction on the ordination, moving from epidermis to stele, there was an increase in PC2 and a decrease in PC3 (bottom left to top right, Fig. 5b). This corresponds to an increase in Zn and Cu while Fe, S, Ca and Na decreased (Table 1). From cell walls to cell interiors generally, there was an increase in PC2, a decrease in PC3 and a slight increase in PC4. Thus from cell walls to cell interiors Zn and Cu increased, Fe, S and Ca decreased, and K and Mg increased slightly (Fig. 5 and Table 1). Among the cytoplasmic granules the trajectory from epidermis to stele also included some increase in K and Mg (from PC4), perhaps because of accumulation of these elements in the stele for transport into leaves and shoots.

Bar graphs provided information on the individual metal distributions (Fig. 6). However, significant interaction terms in analyses of variances demand conservative interpretation of these graphs. Levels of Fe were high in external granules and epidermal cell walls, and levels of Fe decreased centripetally (towards the stele), both in cell walls and inside cells (Fig. 6). The epidermis cytoplasmic granules were also quite rich in Fe (Fig. 6).

For Cu, the highest levels were inside cells in the stele and then cell walls in the stele (Fig. 6). Zn levels were highest inside cells of the stele and increased centripetally in the cell walls (Fig. 6). Trends in Pb distribution were not obvious, but there was a tendency to higher levels centripetally with the highest levels found inside cells of the stele (Fig. 6). Little Cu, Zn and Pb were found in the external granules (Fig. 6).

DISCUSSION

We have reported metal localization in roots of a free-floating aquatic plant, demonstrating metal uptake and confirming that surface adsorption and binding are not solely responsible for the high metal concentrations we previously measured in acid digests of roots of this plant (Vesk & Allaway 1997). We have shown how individual metals differ in their distribution. While Fe (and Al, Mn and Ti)

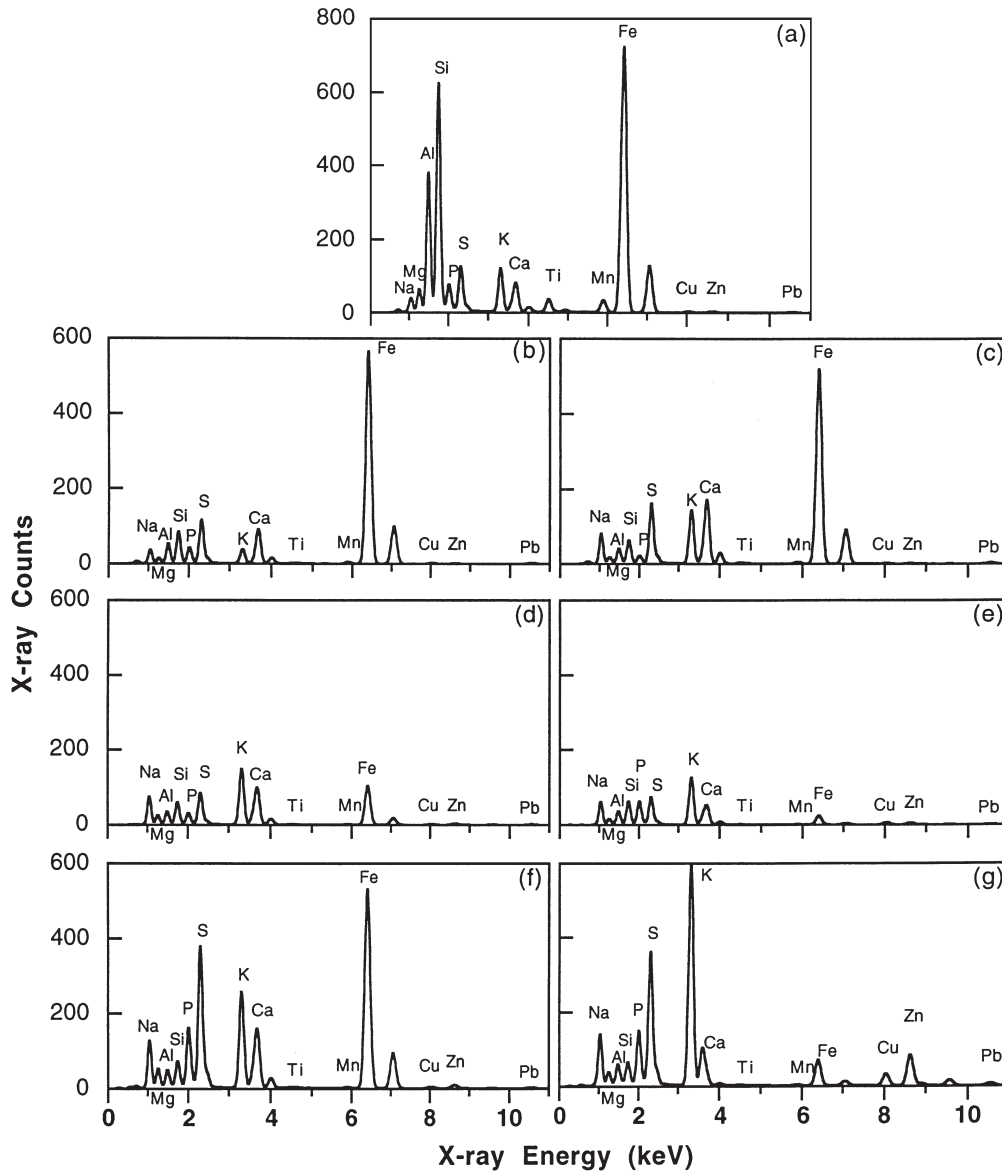


Figure 4. Average X-ray microanalysis spectra for analysis regions in root transverse sections, modelled from mean X-ray intensities from two analyses at each region from one section from each of two roots from each of 18 plants using Desk Top Spectrum Analyzer (see text). Note, no background has been modelled. a, external granules; b, epidermis external walls; c, epidermis internal walls; d, parenchyma internal walls; e, stele internal walls; f, epidermis cytoplasmic granules; g, stele cytoplasmic granules.

was indeed localized at the root surface and decreased towards the root centre, Cu, Zn and Pb were *not* localized at the root surface and *increased* towards the root centre. Cell walls were the major sites of Fe accumulation, while Cu and Zn were mainly localized in electron-dense granules within cells of the stele, with stele cell walls and epidermal cell granules also important.

Iron localization

Iron localization in external granules and the epidermal walls is consistent with reports of plaques of Fe oxyhydroxides formed by oxygen evolution by the roots and

microbial metabolism in a range of rooted emergent and rooted submergent aquatic plants (Green & Etherington 1977; Chen, Dixon & Turner 1980; Mendelsohn & Postek 1982; Taylor, Crowder & Rodden 1984; St-Cyr, Fortin & Campbell 1993). Green & Etherington (1977) also reported Fe within rice roots, extending into the cell walls of the cortical parenchyma with dense deposits of Fe along the middle lamella and in intercellular spaces which they attributed to extracellular oxygen transport (cf. Fig. 2 and Fig. 6). Oxidation is believed to be a mechanism of avoiding toxicity of reduced forms of Fe and Mn to roots under flooded conditions (Green & Etherington 1977; Marschner 1995). The appearance of the root surface of *Eichhornia*

Table 1. Principal components of variation in elemental localization and multiple regression of the principal components to interpret MDS ordination in Fig. 5¹

Principal component	Eigenvalues (λ)	Cumulative percentage variance	Factor loading	Multiple regression statistics		
				$F_{(2,116)}$	P	r^2
PC 1	2.39	17	0.90(Si) + 0.86(Al) + 0.54(Ti)	43.20	<0.0001	0.43
PC 2	2.33	34	0.84(Zn) + 0.83(Cu) - 0.47(Fe)	56.84	<0.0001	0.49
PC 3	1.85	47	0.79(S) + 0.62(Ca) + 0.55(Fe) + 0.47(Na)	10.83	<0.0001	0.16
PC 4	1.6	58	0.85(K) + 0.54(Mg) + 0.50(Na)	25.78	<0.0001	0.31
PC 5	1.25	67	0.79(Mn) + 0.74(P)	0.68	>0.5, NS	0.01

¹Rotated factor loading matrix for the first five principal components from correlation-based PCA of $\log_e(x + 0.001)$ -transformed data from means for each of seven regions in each of 18 plants ($n = 126$ analyses), followed by retaining five principal components, using varimax rotation and reporting only significant loadings (critical value = 0.463, which is a conservative twice the value for $\alpha = 0.01$). Results of multiple regression of the principal component scores of each object (calculated by Factor Loading) on x and y co-ordinates of those objects in the MDS ordination of samples representing the means of each region within each plant for dimensional interpretation of the MDS ordination. A conservative significance level was used to control Type 1 error for the five F -ratio tests of the multiple regressions, using $\alpha = 0.01$, $\alpha' = 0.01/5 = 0.002$. NS, not significant.

crassipes was similar to that in *Typha latifolia* (Taylor *et al.* 1984) and *Spartina alterniflora* roots growing under flooded conditions (Mendelssohn & Postek 1982), suggesting that iron plaques can occur on roots of free-floating aquatic plants too. The occurrence of Fe deposits within epidermal cells, i.e. epidermal cytoplasmic granules (see Fig. 2 and Fig. 6) may be the result of damaged cells and infilling with Fe similar to previous reports of root plaques (Chen *et al.* 1980; Taylor *et al.* 1984).

Finding that Fe and trace metals Cu, Zn and Pb were not colocalized was unexpected. Root plaques have been reported to contain metals in addition to Fe, notably Mn, Cu and Zn (Otte *et al.* 1989; St-Cyr & Crowder 1990; St-Cyr *et al.* 1993; St-Cyr & Campbell 1996; Ye *et al.* 1997).

The effect of the root plaque on uptake and translocation of other metals is a matter of debate, with some authors claiming a regulatory function for the plaque (e.g. Otte *et al.* 1989; Greipsson & Crowder 1992; St-Cyr & Campbell 1996), and others finding no evidence for such a role (Ye *et al.* 1997). The material at the root surface of these free-floating water hyacinth may not be a true root plaque in the sense of wetland plants with roots anchored in the substrate. Even so, deposition of Fe at the root surface did not immobilize trace metals which were found deep within the root. This demonstrates that uptake is significant and the roots do not just provide a surface for particulate adsorption and microbial growth (and physical effects such as flow reduction and sediment settling).

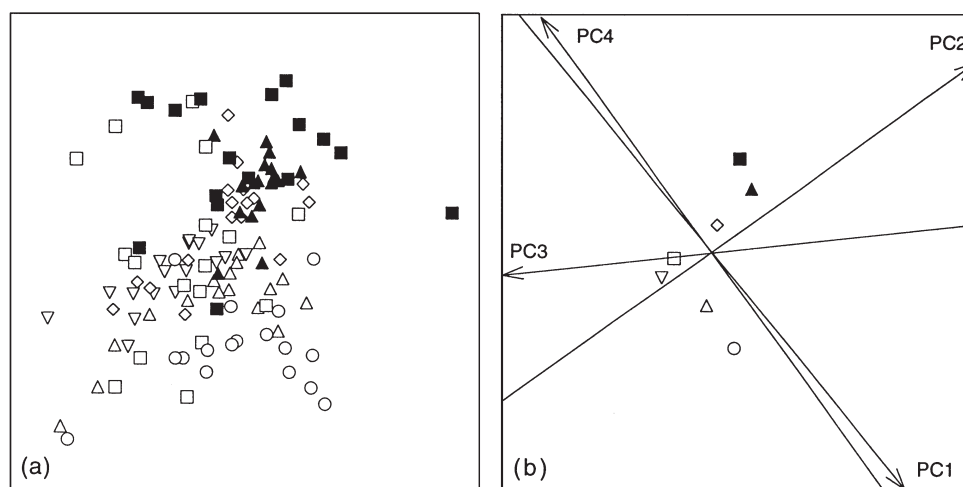


Figure 5. a, Multi-dimensional scaling (MDS) ordination of analysis regions from 17 plants. Each symbol represents the mean of two analyses from each of two roots from one plant, Kruskal's stress = 0.17. Symbols: ○, external granules; △, epidermis external walls; ▽, epidermis internal walls; ◇, parenchyma internal walls; ▲, stele internal walls; □, epidermis cytoplasmic granules; ■, stele cytoplasmic granules. MDS plots are determined with an arbitrary scale, location, rotation and reflection: only relative position is important, hence the plot axes lack scales and labels. b, Dimensional interpretation of the ordination space in (a). Arrows are from multiple linear regression of principal component scores on x and y co-ordinates of the ordination (see Table 1). Symbols represent centroids of regions in (a), i.e. the means of x and y co-ordinates.

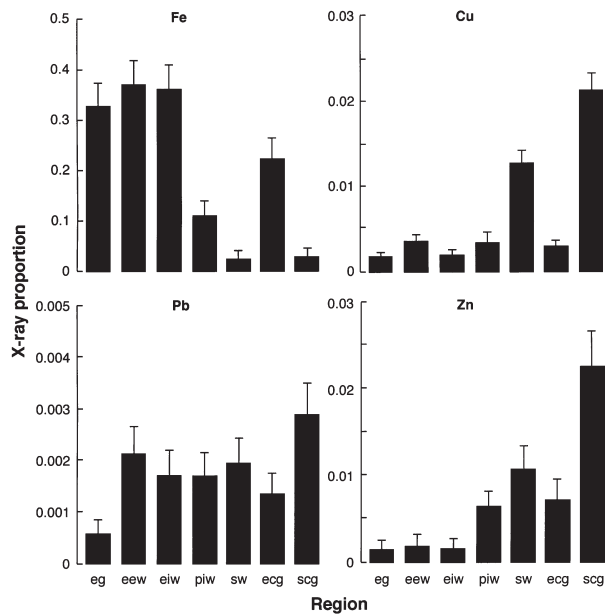


Figure 6. Mean (\pm SEM) X-ray counts for Fe, Cu, Zn and Pb expressed as proportions of all elemental X-rays from two X-ray microanalyses for each region from one transverse section from each of two secondary roots from each of 18 plants (Regions: eg, external granules; eew, epidermis external walls; eiw, epidermis internal walls; piw, parenchyma internal walls; sw, stele internal walls; ecg, epidermis cytoplasmic granules; scg, stele cytoplasmic granules).

General localization of trace metals

Few reports of trace metal localization within roots of plants using X-ray microanalysis exist in the literature, and even fewer dealing with aquatic plants. Sela *et al.* (1988) reported localization of Cu (also Cd and U) in the aquatic fern *Azolla filiculoides* and van Steveninck *et al.* (1990a,b, van Steveninck, van Steveninck & Fernando 1992) have investigated Zn (and Cd) localization in the aquatic angiosperm *Lemna minor*. Other reports have investigated grasses (Mullins *et al.* 1985; van Steveninck *et al.* 1987) and dicotyledonous plants (Mullins *et al.* 1985; van Steveninck *et al.* 1993, 1994), including a hyper-accumulating herb (Vázquez *et al.* 1992) and tree seedlings (Denny & Wilkins 1987; Jentschke, Fritz & Godbold 1991; Arduini, Godbold & Onnis 1996).

Our results showed centripetal increase in Zn with the highest levels in the stele. Previous studies have emphasized Zn localization in parenchyma adjacent to vascular tissue in *L. minor* (van Steveninck *et al.* 1990a), in cortical parenchyma in *Deschampsia caespitosa* (van Steveninck *et al.* 1987), and the endodermis (Denny & Wilkins 1987; van Steveninck *et al.* 1993, 1994). Mullins *et al.* (1985) found that Zn accumulation bodies decreased centripetally in *D. caespitosa* and *Anthoxanthum odoratum*. We found that Cu levels also increased centripetally with the highest levels in the stele. This contrasts with previous reports of a centripetal decrease of Cu levels in roots

of *Fraxinus angustifolia* (Arduini *et al.* 1996), and centripetal decrease in the number of electron-dense vacuolar bodies containing Cu found in *Mimulus guttatus* (Mullins *et al.* 1985).

Lead was found at the highest levels in the stele whereas previous reports have emphasized the cortical parenchyma and endodermis in roots of *Allium cepa* (Wierzbicka 1987) and mycorrhizal roots of *Picea abies* (Jentschke *et al.* 1991). Interestingly, what we called parenchyma internal wall was the outer wall of the endodermis, and it did not contain substantial Pb levels. Our inability to locate substantial levels of Pb was interesting, given the high levels in root digests and limited translocation to leaves compared with Cu (Vesik & Allaway 1997). Two possibilities might explain this; either Pb was localized somewhere we did not analyse, or Pb was not localized but was fairly evenly distributed across the root.

Cellular localization of trace metals

We found Cu and Zn to be mainly localized inside cells, with a lesser but significant amount in the stele cell walls. This is in accordance with a number of reports, mostly describing vacuolar localization (Mullins *et al.* 1985; Denny & Wilkins 1987; van Steveninck *et al.* 1987, 1990b; Vázquez *et al.* 1992). Arduini *et al.* (1996) however, found that in *F. angustifolia* Cu was strongly accumulated within the cell walls of the cortex. Sela *et al.* (1988) also found Cu accumulation in cell walls compared with cell lumen, although this may reflect their sampling of 'cytoplasm', compared with our selection of electron opaque granules. Within cells we found that Cu, Zn and Pb were often associated with the anionic elements P and/or S. Association with P (and also K) would be consistent with binding by phytic acid (van Steveninck *et al.* 1987, 1990a, 1993, 1994), while association with both P and S would be expected in phytochelatin binding (Steffens 1990; van Steveninck *et al.* 1990b, 1992; El-Enany & Mazen 1996). Mullins *et al.* (1985) also reported Cu, Zn and Pb in electron-dense bodies with S, Ca & P. Denny & Wilkins (1987) reported a similar result for Zn and concluded that the granules were amorphous and proteinaceous. Lead has been reported to be mainly distributed apoplastically for a range of species including onion roots (Wierzbicka 1987); Norway spruce roots (*Picea abies*) (Jentschke *et al.* 1991); *Potamogeton* leaves (Sharpe & Denny 1976); although Mullins *et al.* (1985) reported both cell walls and electron dense vacuolar bodies as being localizations of Pb in *Anthoxanthum odoratum*.

Implications of this research

The marked localization of the trace elements in the stele would be consistent with acropetal translocation of Cu, Zn and Pb and raises the question of why then, the leaf concentrations of Cu and Pb in water hyacinth measured with

atomic absorption spectrometry were so low (Vesk & Allaway 1997). A possible explanation could be that the translocated elements are distributed at a low concentration over a large biomass. Limited mobility of Cu with high retention in roots has been reported by a number of authors (Jarvis & Whitehead 1981; Lepp, Dickinson & Ormand 1984; Sela *et al.* 1988). Perhaps there are losses to binding during xylem transport through the stems or accumulation in xylem parenchyma (Fernandes & Henriques 1991; Marschner 1995: p.83).

The differential localization of metals within the roots may be important in determining how well the metals may be bound and released on senescence of the plants. Formation of metal complexes, for instance through coprecipitation on Fe oxyhydroxides would lead to transfer of those metals to the sediment. Cell walls tend to break down more slowly than other components (Suren 1989) and their breakdown also exposes new binding sites for metals. As a result, cell wall-bound metals may be exported from a wetland to a lesser extent (or later) than those metals bound intracellularly. A metal budget study of a fluvial lake in Canada found that export of Al, Fe and Mn from a macrophyte bed was depressed compared with that of Cu, Cr, Ni and Zn (Jackson *et al.* 1994). Jackson *et al.* (1994) suggested binding of Al, Fe and Mn in cell walls to explain the reduced export and our metal localization results support this.

The present study has demonstrated the complexity and variability of metal localization in field collected plants exposed to a gradient of metal levels (Vesk & Allaway 1997). We sampled extensively with replication at a number of hierarchical levels to gain understanding of the scale of patterns and their consistency or otherwise in the field. High variability at each level of sampling led to interactions in analyses of variance. This meant that the patterns as presented in Fig. 6 were not strictly consistent. Accordingly caution is recommended in interpreting these patterns. The structural and functional heterogeneity of the root and cells militates against identification of clear simple patterns, and we therefore emphasize the need for comprehensive sampling designs and field sampling to address questions of metal localization.

Despite the variability some patterns have been identified. Contrary to a number of studies we have found centripetal increases in trace metal concentration. This work may contribute to improved understanding of the relationships between metal concentrations in plants and their environment, which underpin biomonitoring and metal flux studies.

ACKNOWLEDGMENTS

This paper is based on work for a MSc thesis by P.A.V. We wish to acknowledge: the University of Sydney and the Australian Research Council for research funds; the Electron Microscope Unit for research facilities and office space for P.A.V.; Peter G. Fairweather and Marti J. Anderson for advice on multivariate statistics; and two reviewers for comments on an earlier draft.

REFERENCES

- Arduini I., Godbold D.L. & Onnis A. (1996) Cadmium and copper uptake and distribution in Mediterranean tree seedlings. *Physiologia Plantarum* **97**, 111–117.
- Beck M.W. (1997) Inference and generality in ecology: current problems and an experimental solution. *Oikos* **78**, 265–273.
- Brix H. & Schierup H.H. (1989) The use of aquatic macrophytes in water-pollution control. *Ambio* **18**, 100–107.
- Brune A., Urbach W. & Dietz K.-J. (1994) Compartmentation and transport of zinc in barley primary leaves as basic mechanisms involved in zinc tolerance. *Plant, Cell and Environment* **17**, 153–162.
- Chen C.C., Dixon J.B. & Turner F.T. (1980) Iron coatings on rice roots: morphology and models of development. *Soil Society of America Journal* **44**, 1113–1119.
- Clarke K.R. (1993) Non-parametric multivariate analyses of changes in community structure. *Australian Journal of Ecology* **18**, 117–143.
- Clarke K.R. & Green R.H. (1988) Statistical design and analysis for a 'biological effects' study. *Marine Ecology Progress Series* **46**, 213–226.
- Denny H.J. & Wilkins D.A. (1987) Zinc tolerance in *Betula* spp. II. Microanalytical studies of zinc uptake into root tissues. *New Phytologist* **106**, 525–534.
- Dunbabin J.S. & Bowmer K.H. (1992) Potential use of constructed wetlands for treatment of industrial wastewaters containing metals. *Science of the Total Environment* **111**, 151–168.
- El-Enany A.E. & Mazen A.M.A. (1996) Isolation of Cd-binding protein of water hyacinth (*Eichhornia crassipes*) grown in Nile River water. *Water, Air and Soil Pollution* **87**, 357–362.
- Ellis J.B., Shutes R.B., Revitt D.M. & Zhang T.T. (1994) Use of macrophytes for pollution treatment in urban wetlands. *Resources, Conservation and Recycling* **11**, 1–12.
- Ernst W.H.O., Verkleij J.A.C. & Schat H. (1992) Metal tolerance in plants. *Acta Botanica Neerlandica* **41**, 229–248.
- Fernandes J.C. & Henriques F.S. (1991) Biochemical, physiological, and structural effects of excess copper in plants. *The Botanical Review* **57**, 246–273.
- Green M.S. & Etherington J.R. (1977) Oxidation of ferrous iron by rice (*Oryza sativa* L.) roots: a mechanism for waterlogging tolerance? *Journal of Experimental Botany* **28**, 678–690.
- Greipsson S. & Crowder A.A. (1992) Amelioration of copper and nickel toxicity by iron plaque on roots of rice (*Oryza sativa*). *Canadian Journal of Botany* **70**, 824–830.
- Jackson L.J., Rasmussen J.B. & Kalff J. (1994) A mass balance analysis of trace metals in two weedbeds. *Water, Air and Soil Pollution* **75**, 107–119.
- Jarvis S.C. & Whitehead D.C. (1981) The influence of some soil and plant factors on the concentration of copper in perennial ryegrass. *Plant and Soil* **60**, 275–286.
- Jentschke G., Fritz E. & Godbold D.L. (1991) Distribution of lead in mycorrhizal and non-mycorrhizal Norway spruce seedlings. *Physiologia Plantarum* **81**, 417–422.
- Joy D.C. (1995) *Monte Carlo Modelling for Electron Microscopy and Microanalysis*. 224 pp. Oxford University Press, Oxford.
- Kruskal J.B. & Wish M. (1978) *Multidimensional Scaling*. 93 pp. Sage Publications, Beverley Hills, London.
- Langston W.J. & Spence S.K. (1994) Metal Analysis. In: *Handbook of Ecotoxicology* (ed. P. Calow), Vol. 2. pp. 45–78. Blackwell Scientific Publications, Oxford.
- Lee T.A. & Hardy J.K. (1987) Copper uptake by the water hyacinth. *Journal of Environmental Science and Health, Series A* **22**, 141–160.
- Lepp N.W., Dickinson N.M. & Ormand K.L. (1984) Distribution of fungicide-derived copper in soils, litter and vegetation of differ-

- ent aged stands of coffee (*Coffea arabica* L.) in Kenya. *Plant and Soil* **77**, 263–270.
- Manly B.F.J. (1994) *Multivariate Statistical Methods, A Primer*. 215 pp. 2nd edn. Chapman & Hall, London, Melbourne.
- Markert B. (1995) Sample preparation (cleaning, drying, homogenization) for trace element analysis in plant matrices. *Science of the Total Environment* **176**, 45–61.
- Marschner H. (1995) *Mineral Nutrition of Higher Plants*. 889 pp. 2nd edn. Academic Press, London.
- Marshall A.T. (1980) Freeze-substitution as a preparation technique for biological X-ray microanalysis. *Scanning Electron Microscopy* **II**, 395–408.
- Mendelssohn I.A. & Postek M.T. (1982) Elemental analysis of deposits on the roots of *Spartina alterniflora* Loisel. *American Journal of Botany* **69**, 904–912.
- Morgan A.J. (1980) Preparation of Specimens: Changes in Chemical Integrity. In *X-Ray Microanalysis in Biology* (ed. M.A. Hayat), pp. 207–239. University Park Press, Baltimore, USA.
- Mullins M., Hardwick K. & Thurman D.A. (1985) Heavy metal location by analytical electron microscopy in conventionally fixed and freeze-substituted roots of metal tolerant and non tolerant ecotypes. In *Proceedings of an International Conference on Heavy Metals in the Environment, Athens, September 1985* (ed. T.D. Lekkas), Vol. 2. pp. 43–46. CEP Consultants, Edinburgh.
- Norman G.R. & Streiner D.L. (1994) *Biostatistics: the bare essentials*. 260 pp. Mosby, St. Louis, MO.
- Orlovich D.A. & Ashford A.E. (1995) X-ray microanalysis of ion distribution in frozen salt/dextran droplets after freeze-substitution and embedding in anhydrous conditions. *Journal of Microscopy* **180**, 117–126.
- Otte M.L., Rozema J., Koster L., Haarsma M.S. & Broekman R.A. (1989) Iron plaque on roots of *Aster tripolium* L.: interaction with zinc uptake. *New Phytologist* **111**, 309–317.
- Outridge P.M. & Noller B.N. (1991) Accumulation of toxic trace elements by freshwater vascular plants. *Reviews of Environmental Contamination and Toxicology* **121**, 2–63.
- Phillips D.J.H. (1994) Bioaccumulation. In *Handbook of Ecotoxicology* (ed. P. Calow), Vol. 1. pp. 378–396. Blackwell Scientific Publications, Oxford.
- Sela M., Tel-Or E., Fritz E. & Huttermann A. (1988) Localization and toxic effects of cadmium, copper and uranium in *Azolla*. *Plant Physiology* **88**, 30–36.
- Sharpe V. & Denny P. (1976) Electron microscope studies on the absorption and localization of lead in the leaf tissue of *Potamogeton pectinatus* L. *Journal of Experimental Botany* **27**, 1155–1162.
- St-Cyr L. & Campbell P.G.C. (1996) Metals (Fe, Mn, Zn) in the root plaque of submerged aquatic plants collected *in situ*: – Relations with metal concentrations in the adjacent sediments and in the root tissue. *Biogeochemistry* **33**, 45–76.
- St-Cyr L., Campbell P.G.C. & Guertin K. (1994) Evaluation of the role of submerged plant beds in the metal budget of a fluvial lake. *Hydrobiologia* **291**, 141–156.
- St-Cyr L. & Crowder A.A. (1990) Manganese and copper in the root plaque of *Phragmites australis* (Cav.) Trin. ex Steudel. *Soil Science* **149**, 191–198.
- St-Cyr L., Fortin D. & Campbell P.G.C. (1993) Microscopic observations of the iron plaque of a submerged aquatic plant (*Vallisneria spiralis* Michx.). *Aquatic Botany* **46**, 155–167.
- Steffens J.C. (1990) The heavy metal-binding peptides of plants. *Annual Review of Plant Physiology and Plant Molecular Biology* **41**, 553–575.
- Suren A.M. (1989) Histological changes in macrophyte tissue during decomposition. *Aquatic Botany* **33**, 27–40.
- Taylor G.J., Crowder A.A. & Rodden R. (1984) Formation and morphology of an iron plaque on the roots of *Typha latifolia* L. grown in solution culture. *American Journal of Botany* **71**, 666–675.
- Thornton B. & Macklon A.E.S. (1989) Copper uptake by ryegrass seedlings; contribution of cell wall adsorption. *Journal of Experimental Botany* **40**, 1105–1111.
- van Steveninck R.F.M., Babare A., Fernando D.R. & van Steveninck M.E. (1993) The binding of zinc in root cells of crop plants by phytic acid. *Plant and Soil* **155/156**, 525–528.
- van Steveninck R.F.M., Babare A., Fernando D.R. & van Steveninck M.E. (1994) The binding of zinc, but not cadmium, by phytic acid in roots of crop plants. *Plant and Soil* **167**, 157–164.
- van Steveninck R.F.M., van Steveninck M.E. & Fernando D.R. (1992) Heavy-metal (Zn, Cd) tolerance in selected clones of duck weed (*Lemna minor*). *Plant and Soil* **146**, 271–280.
- van Steveninck R.F.M., van Steveninck M.E., Fernando D.R., Horst W.J. & Marschner H. (1987) Deposition of zinc phytate in globular bodies in roots of *Deschampsia caespitosa* ecotypes; a detoxification mechanism? *Journal of Plant Physiology* **131**, 247–257.
- van Steveninck R.F.M., van Steveninck M.E., Wells A.J. & Fernando D.R. (1990a) Zinc tolerance and the binding of zinc as zinc phytate in *Lemna minor*. X-ray microanalytical evidence. *Journal of Plant Physiology* **137**, 140–146.
- van Steveninck R.F.M., van Steveninck M.E., Fernando D.R., Edwards L.B. & Wells A.J. (1990b) Electron probe X-ray microanalytical evidence for two distinct mechanisms of Zn and Cd binding in a Zn tolerant clone of *Lemna minor* L. *Comptes Rendus de l'Academie Des Sciences. Serie III, Sciences de la Vie* **310**, 671–678.
- Vázquez M.D., Barceló J., Poschenrieder C., Mádico J., Hatton P., Baker A.J.M. & Cope G.H. (1992) Localization of zinc and cadmium in *Thlaspi caerulescens* (Brassicaceae), a metallophyte that can hyperaccumulate both metals. *Journal of Plant Physiology* **140**, 350–355.
- Vesk P.A. & Allaway W.G. (1997) Spatial variation of copper and lead concentrations of water hyacinth plants in a wetland receiving urban run-off. *Aquatic Botany* **59**, 33–44.
- Whitton B.A. & Kelly M.G. (1995) Use of algae and other plants for monitoring rivers. *Australian Journal of Ecology* **20**, 45–56.
- Wierzbicka M. (1987) Lead accumulation and its translocation boundaries in the roots of *Allium cepa* L. – autoradiographic and ultrastructural studies. *Plant, Cell and Environment* **10**, 17–26.
- Ye, Z. H., Baker A.J.M., Wong M.H. & Willis A.J. (1997) Copper and nickel uptake, accumulation and tolerance in *Typha latifolia* with and without iron plaque on the root surface. *New Phytologist* **136**, 481–488.

Received 3 May 1998; received in revised form 17 August 1998; accepted for publication 17 August 1998